

# Array Amplification in Cellular System for 5G Communication

SrihariChintha, Research Scholar , Department of Computer Science & Engineering,  
Sunrise University, Alwar, Rajasthan

Dr.SudhirDawra, (Supervisor), Department of Computer Science & Engineering, Sunrise University,  
Alwar, Rajasthan

**Abstract:** The mobile communication systems utilizing spectrum range of 300MHz-3GHz. The millimeter wave broadband (MMB) system introduced for 5G cellular. The design and operation of future fifth generation cellular networks that use the mm wave spectrum. In this paper the measurements for outdoor cellular channel at 28 GHz was made in urban environment with broadband sliding correlator channel sounder. The angle of arrival, path loss and multipath time delay spread measurements were conducted for steerable beam antennas for finding the location of transmitter and receivers.

**Key words:** 5G • Millimeter wave propagation measurement • MIMO • 28GHz • AOA

## INTRODUCTION

The millimeter wave region of electromagnetic spectrum corresponds to radio band frequencies of 30GHz to 300GHz sometimes called Extremely high frequency (EHF) range. One of the greatest and most important uses of millimeter wave is in transmitting large amount of data. Millimeter wave can achieve multi gigabit data rates at a distance up to few kilometers exist for point to point communication.

**Millimeter Wave Spectrum:** The radio communications such as high definition TV, cellular AM/FM radio, satellite communication, GPS Wi-Fi have been contained in a narrow band of the RF spectrum in 300MHz-3GHz. This type of band is known as swept spot. The use of Ultra wide band in the range of 3.1-10.6GHz which is used to enable high data rate connectivity in personal area networks.

The use of 57-64GHz oxygen absorption band is also used to provide multi gigabit data rates for short range connectivity and wireless local area networks [1]. Local multipoint distribution service (LMDS) operating the frequency ranging from 28 to 30 GHz treated as a broadband fixed wireless, point to multipoint technology.

The frequency ranging from 57-64 GHz oxygen absorption band can experience attenuation of about 15 Db/km as the oxygen molecule (O<sub>2</sub>) absorbs electromagnetic energy at 60GHz [1]. LMDS was

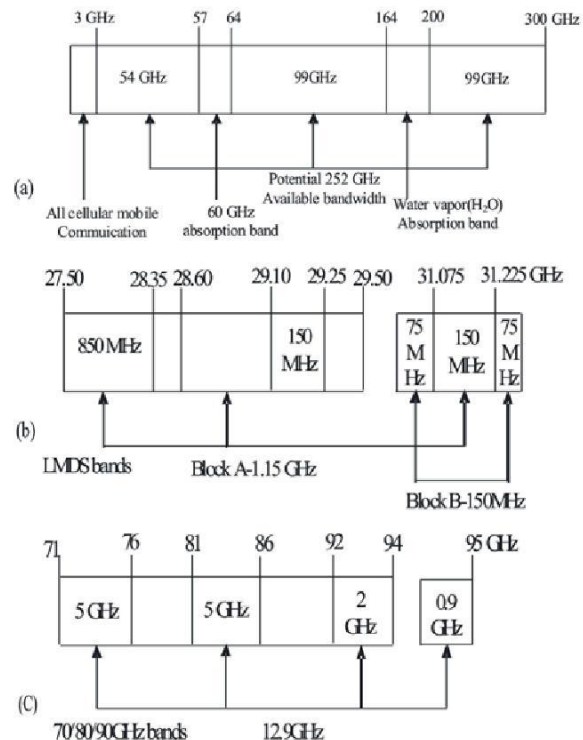


Fig. 1: Millimeter wave spectrum

standardized by IEEE 802 LAN /MAN standards committee through the efforts of IEEE 802.16.1 task group LMDS provide multiple (base) stations supporting point

to multipoint communication to small customer transceivers. A license includes a 1.15 GHz bandwidth and consists of the 27.5-28.35 GHz, 29.1-29.25 GHz and 31.075-31.225 GHz bands. The B license is 150MHz wide consists of 31.0- 31.075 GHz and 31.225-31.3 GHz bands.

**5G Mobile Communications:** The 0G system technologies included PTT (push to talk), MTS (mobile telephone system, IMTS (improved mobile telephone service, AMTS (advanced mobile telephone system. 0G was proved wrong in 1990-91 in Finland. Generally 1G was old analog system the supporting speed up to 2.4kbps. Advanced mobile phone system (AMPS) was launched by US and is a 1G mobile systems. 2G cellular was launched on the GSM standard in Finland in 1991. 2G services are text messages. Picture messages and MMS (multimedia messages). 2G used for voice transmission with digital signal speed up to 64kbps. 2G are used either Time division multiple access (TDMA) or Code division multiple access (CDMA). TDMA technologies are GSM.PDC, Iden, IS-

136. CDMA technology is IS-95. GSM technology establish international roaming. International mobile telecommunications advanced (IMT-Advanced) standard is 3G [2].

The 3G is able to transmit packet data switch at increased bandwidth. The 3G having transmission speed from 125kbps to 2Mbps. 3G used in computer networking (WCDMA, WLAN & Bluetooth). 3G mobile includes fast communication, internet, mobile T.V, video conferencing, video calls, multi media messaging service(MMS), 3D gaming, multigaming etc. 4G is high speed wireless network. 4G should be able to give very smooth global roaming with lower cost. 4G is fast data transfer rates. 4G includes multiple input and multiple output (MIMO) [3] Which enables multistream transmission for high spectrum efficiency, improved link quality, radiation pattern obtained via adaptive beam forming antenna arrays.

4G will use of much greater spectrum allocations at mm-wave frequency bands, applications of mobile TV a provider redirects a TV channel directly to the subscriber's phone. Mobile ultra broadband (gigabit speed) access and multi carrier transmission. 4G also used as mobile WIMAX (worldwide interoperability) for microwave access. LTE and WIMAX are the part of 4G. WIMAX and long term Evolution (LTE) the standard generally accepted to succeed both CDMA and GSM. WIMAX and LTE range between 4Mbps and 30 Mbps. 4G wireless networks designed primarily for data, IP based protocols (LTE) and true mobile broadband.

5G technologies include all type of advanced features. 5G which provides much greater spectrum allocations at mm wave spectrum using highly directional beam forming antenna.

**MillimeterWave Mobile Communication for 5G:** Mobile data rates expand to the multigiga bit per second range by using steerable antenna and mm wave spectrum which simultaneously support mobile communications with convergence of cellular and Wi-Fi services. mm carrier frequencies used for large bandwidth allocations which transfer high data rates. mm wave frequencies provide polarization and spatial processing techniques such as massive MIMO and adaptive Beamforming [3].

**MIMO:** Multiple-input multiple-output (MIMO) technology is maturing and is being incorporated into emerging wireless broadband standards like long-term evolution (LTE). For example, the LTE standard allows for up to eight antenna ports at the base station. Basically, the more antennas the transmitter/receiver is equipped with and the more degrees of freedom that the propagation channel can provide, the better the performance in terms of data rate or link reliability. More precisely, on a quasistatic channel where a codeword spans across only one time and frequency coherence interval, the reliability of a point-to-point MIMO link scales according to Prob (linkoutage) SNR-ntnr.

#### Literature Survey

##### Antenna and Propagation Aspects of Very Large

**MIMO:** The performance of all types of MIMO systems strongly depends on properties of the antenna arrays and the propagation environment in which the system is operating. The complexity of the propagation environment, in combination with the capability of the antenna arrays to exploit this complexity, limits the achievable system performance. When the number of antenna elements in the arrays increases, that meet both opportunities and challenges. The opportunities include increased capabilities of exploiting the propagation channel, with better spatial resolution. With well-separated ideal antenna elements, in a sufficiently complex propagation environment and without directivity and mutual coupling, each additional antenna element in the array adds another degree of freedom that can be used by the system. In reality, though, the antenna elements are never ideal, they are not always well separated and the

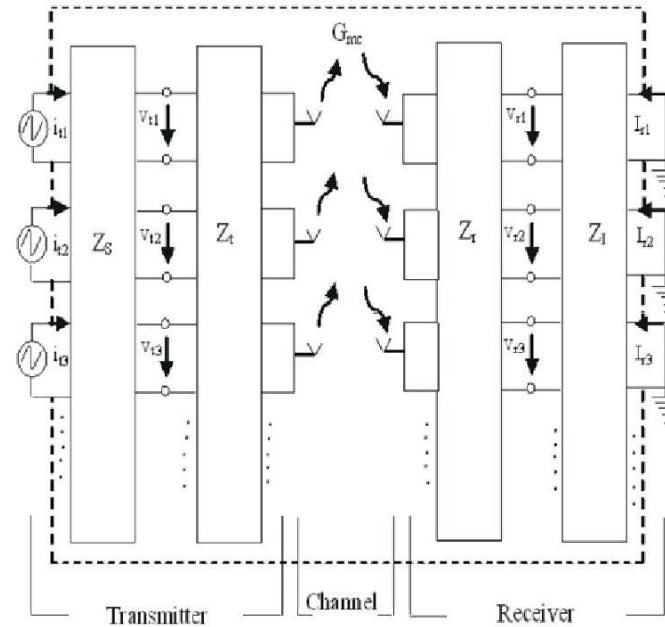


Fig. 2: MIMO systems with antenna impedance matrices and matching networks

propagation environment may not be complex enough to offer the large number of degrees of freedom that a large antenna array could exploit.

In this section, this illustrates and discusses some of these opportunities and challenges, starting with an example of how more antennas in an ideal situation improve our capability to focus the field strength to a specific geographical point (a certain user). This is followed by an analysis of how realistic (nonideal) antenna arrays influence the system performance in an ideal propagation environment. Finally, the use of channel measurements to address properties of a real case with a 128-element base station array serving six single-antenna users [2].

**Broadband Millimeter-wave Propagation Measurements and Models:** Understanding radio propagation is vital for the Successful design and implementation of new wireless communication systems operating at higher frequencies and bandwidths. The advancement of sub-terahertz (THz)

[2] semiconductor technology has now made millimeter-wave cellular systems feasible [2]. While outdoor channel measurements at millimeter-wave frequencies (e.g., frequencies above 30 GHz, or wavelengths 10 mm or less) have been conducted by many (for example, rain attenuation foliage attenuation multipath delay spread angle of arrival (AOA); reflection coefficients of materials and coverage outage probability, past work has been done for either ground level or fixed point (i.e., 28 GHz

LMDS) wireless communications. Previous researchers have not considered the propagation of millimeter waves using steerable antennas for cellular/mobile applications [3-5].

This paper provides a comprehensive propagation study for outdoor urban millimeter wave (e.g., sub-THz) cellular networks with beam steering. Our work considers a variety of elevated transmitters that represent typical fifth-generation (5G) base-station locations at heights of two or more stories above ground level and dozens of ground-level receiver locations. Highly directional steerable horn antennas at the transmitter and receiver were used to measure the propagation channel for angle of arrival (AOA), [6] multipath time delay spread and propagation path loss.

An 800-MHz null-to-null pass band bandwidth spread-spectrum sliding correlate channel sounder similar to that used in [4] and was built to perform extensive outdoor cellular millimeter-wave propagation measurements at 37.625-GHz [2] center frequency. An RF signal power of 22 dBm was delivered to the transmit base-station antenna, which was a 7.8 half-power beam width Ka-band vertically polarized 25-dBi horn antenna to produce 47-dBm EIRP The receiver uses another Ka-band vertically polarized horn antenna of either 13.3-dBi gain (49.4 beam width), or 25-dBi gain (7.8 beam width). The idea of using beam steering to form links within cellular networks is not new but past work has not considered the use of millimeter-wave spectrum and the

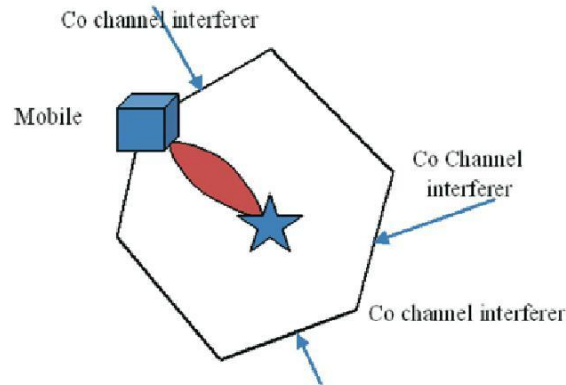


Fig. 3: Use of highly directional receiver antenna system

additional capabilities of small form factor steerable antennas at the handset and base station for mobile/cellular use. Moving to the millimeter-wave spectrum would provide orders of magnitude of available spectrum to cellular carriers when compared to today's global 4G allocation, while simultaneously supporting in bandbackhaul [7-9].

Spatial-division multiple access (SDMA) and beam/path combining could be utilized along with temporal or frequency-based multiple-access techniques to greatly increase capacity and spectrum reuse. A cell tower [10] coverage region is broken into six sectors of 60 each, which yields at least a 5 increase in the number of users that a cell site can handle. The benefits provided by spatial-division multiple-access (SDMA) systems include an extended range due to high gain antennas, reduced interference by intelligently controlling the beam direction and increased cell capacity. The Problem of intercell interference, which currently plagues dense heterogeneous network deployments, would be significantly reduced with the use of highly directional steerable beam antenna arrays at the mobile and/or base station.

As illustrated in Figure 1, interference becomes less likely due to the narrow beam width at the base station. Thus, millimeter-wave cellular systems are most likely to be noise limited at heavily shadowed locations rather than limited by interference. The use of small directional antennas leads to a new research field of antenna pointing protocols.

Early work on millimeter-wave antenna pointing protocols appears in and is based on iterative antenna training using pseudo noise sequences. Additional millimeter-wave protocols for pointing antennas at both base station and mobile handsets were recently presented

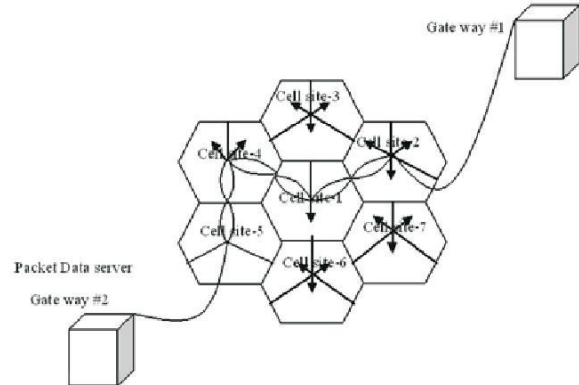


Fig. 4: Cell systems may use steerable antenna Array

in and through use of narrowband pilot signals, antenna pointing directions and multipath angular spreads can be rapidly determined.

**Understanding the Channel:** Future wireless technologies must be validated in the most urban environments, such as New York City. In order to improve capacity and service quality, the cellular network architecture needs to support higher spatial reuse. Massive MIMO [2] base stations and small-cell access points are two promising approaches for future cellular. Massive MIMO base stations allocate antenna arrays at existing macro base stations, which can accurately concentrate transmitted energy the mobile users. Small cells offload traffic from base stations by overlaying a layer of small cell access points, which actually decreases the average distance between transmitters and users, resulting in lower propagation losses and higher data rates and energy efficiency. Both of these important trends are readily supported and, in fact, are enhanced by a move to mm-wave spectrum, since the tiny wavelengths allow for dozens to hundreds of antenna elements to be placed in an array on a relatively small physical platform at the base station, or access point and the natural evolution to small cells ensures that mm-wave frequencies will overcome any attenuation due to rain. Understanding the radio channel is a fundamental requirement to develop future mm-wave mobile systems as well as backhaul techniques. In order to create a statistical spatial channel model (SSCM) [8] for mm-wave multipath channels, extensive measurements must be made in typical and worst-case operating conditions and environments [1].

**28 GHZ Broadband Channel Sounding Hardware:** Using a 400 Mcps sliding correlator channel sounder with 2.3ns multipath resolution, conducted extensive mm wave

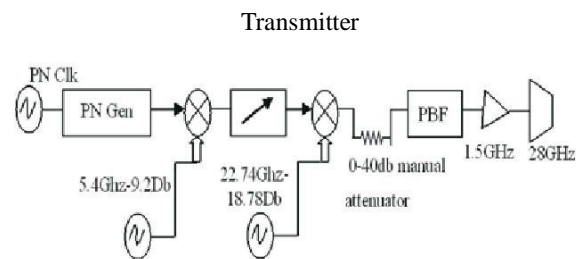


Fig. 5: TX the mm wave propagation measurement at 28 GHz

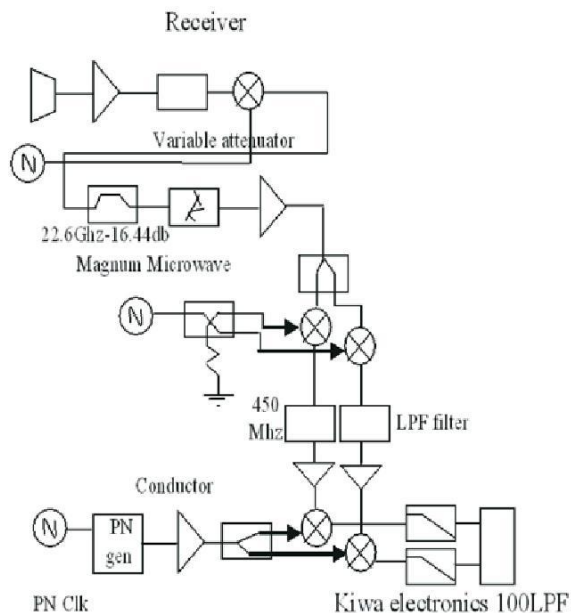


Fig. 6: RX for the mm wave measurement at 28 GHz

propagation measurements at 28 GHz in 2012. The block diagram of the transmitter (TX) and receiver (RX) is given in Figure 5. A pseudo-random noise (PN) sequence sliding correlator was utilized as the probing signal, which was modulated to a 5.4 GHz intermediate frequency (IF) and upconverted to 28 GHz after mixing with a 22.6 GHz local oscillator (LO).

The transmitter power was +30 dBm (a typical value for lower power femtocells), fed to a steerable 10° beam width 24.5 dBi horn antenna or a 30° beam width 15 dBi of horn antennas was mechanically rotated. In order to achieve increased measurement dynamic range for increased coverage distance, we used a sliding correlator spread spectrum system. Total measured dynamic range was approximately 178 dB between the transmitter and receiver using the most directional horn antennas in order to obtain an SNR of 10 dB, on the order of future small cells. All propagation measurement equipment used AC power outlets that were available from various buildings,

thus avoiding Beam width 24.5 dBi horn antennas or a 30 beam width 15 dBi horn antenna that was mechanically rotated. The receiver used the battery depletion problem.

**28GHz Building Penetration and Reflection Measurement:** To understand the mm-wave propagation environment in urban areas, signal penetration and reflection properties of common building materials with typical smooth and rough surfaces are required for both indoor and outdoor cases. We conducted penetration and reflection measurements at 28 GHz throughout the summer of 2012.

#### **Analysis of Millimeter Wave Measurement**

**38 GHz Broadband Channel Sounding Hardware and Measurement Procedure:** An 800 MHz null-to-null bandwidth spread spectrum sliding correlator channel sounder was employed in the 38 GHz propagation measurement campaign in Austin. The PN sequence was operating at 400 Mcps and 399.9 Mcps at the TX and RX, respectively, to offer a slide factor of 8000 and adequate processing gain. The PN sequence was modulated by a 5.4 GHz IF signal, which was input into the up converter that contained LO frequency multipliers to generate a carrier frequency of 37.625 GHz with a +22 dBm output power before the TX antenna. A 25-dBi gain Ka-band vertically polarized horn antenna with 7.8 half-power beam width was utilized at the TX and an identical antenna (and also a wider beam 13.3-dBi gain (49.4 beam width) vertically polarized horn antenna) were used at the RX. The maximum measurable path loss was about 160 dB. 38GHz cellular propagations measurements were conducted in Austin. The RX was positioned in a number of LOS, partially obstructed LOS and NLOS locations representative of an outdoor urban environment including foliage, high-rise buildings and pedestrian and vehicular traffic. At each receiver location, measurements were acquired using a circular track with 8 equally spaced local area measurement points separated by 45 increments. The radius of the circular track yielded a 10 separation distance between consecutive points along the circular track. For LOS links, the TX and RX were pointed directly at each other in both azimuth and elevation. The captured PDPs for each complete track measurement were then averaged and a new RX location was selected. NLOS conditions were taken over the circular track and a subsequent 360 azimuth exhaustive signal search was conducted [3].

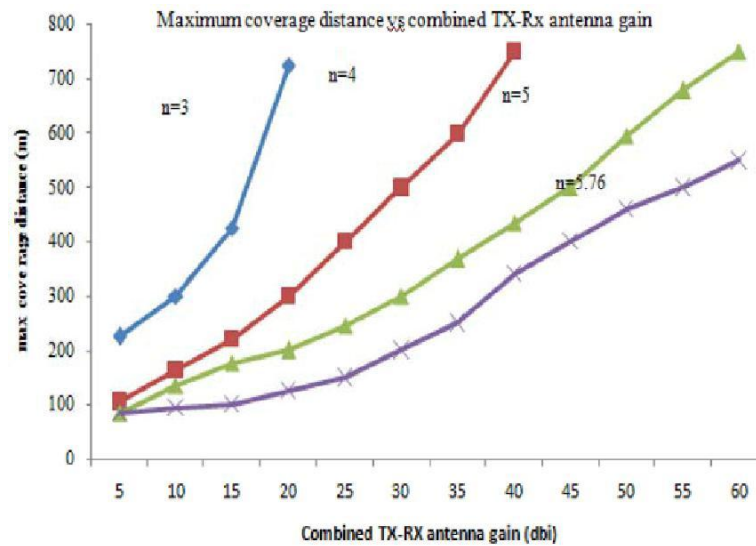


Fig. 7: Maximum coverage distances at 28 GHz with 119 dB maximum path loss dynamic range

### Cellular Urban Measurement Results

**AOA Distributions:** AOA distributions were generated for each transmitter location (e.g., base station). We defined a link as being any signal with lower path loss than 160 dB, which is the maximum measured by the channel sounder system. A scatter plot showing all of the receiver and transmitter azimuth angle combinations for all links made at the WRW-A transmitter location is shown in Figure 5. The right side of contains a histogram of the number of links for each receiver azimuth angle in 10 incremental bins. The bottom of shows the distribution of transmitter azimuth angles. Only measurements performed with the 25-dBi RX antenna are included in the azimuth angle histograms since the narrower beam is better suited for AOA information. The 13.3-dBi RX antenna measurements were conducted in the same locations and yielded similar results, although the number of observed links was slightly less due to a broader beam width that could not resolve individual links and 12 dB less link budget.

**Propagation Path Loss:** Path loss was extracted for every measured multipath component (e.g., link) made with every unique pair of transmitter and receiver pointing angles across the 43 measurement locations. For each measured link, the radio path was identified as clear LOS for an unobstructed path when the TX and RX antennas were pointing at each other, partially obstructed LOS [6] with some physical obstructions when the beams were pointed at each other and NLOS links where antennas were pointed off bore sight, thereby exploiting reflections. Path loss scatter plots were modeled using the standard

log-normal shadowing model where the measured path loss data was fitted with a MMSE best-fit path loss exponent. The log-normal shadowing model is given by (1), where the path loss is in dB and is a function of distance and assumed to be a random value. Path loss is related to a close-in free-space reference distance, 5m and is modeled by the path loss exponent and a shadowing random variable which is represented as a Gaussian random variable in dB with zero mean and dB standard deviation [11-15].

$$PL(d) = PL(d_0) + 10n * \log(d) + \chi_0$$

The log-normal shadowing model has been used to model any arbitrary link without consideration of antenna characteristics. However, the introduction of steerable and highly directional antennas leads to a significant dependence of the path-loss exponent and on antenna orientations. Since TX and RX antennas were pointed at a wide range of angles, we considered radio propagation path loss for two cases: one case was when TX and RX antennas had a visible line of sight between each other and were pointed at each other (LOS-directed), [14] and the other case was when the RX and TX antennas did not have a visible LOS due to obstructions and were not pointed at each other so that reflections or scattering could be used to make a NLOS link (NLOS-directed).

LOS- directed antennas consistently had lower path loss than NLOS, even in cases with partially obstructed LOS link due to foliage or edges of buildings.

Table 1: Path loss exponents and Standard Deviation for All 38 GHz Cellular Measurements with Steerable TX and Rx Antennas [11],[4]

	25 dBi RX Ant		13.3 dBi RX Ant	
	LOS	NLOS	LOS	NLOS
Path Loss Exponent n	2.20 (clear 1.92)	3.88 (best 3.13)	2.21 (clear 1.90)	3.18 (best 2.56)
Path Loss $\sigma$ (dB)	10.3 (clear 5.1)	14.6 (best 10.7)	9.4 (clear 3.5)	11.0 (best 8.4)

LOS:Line of Sight

NLOS: Non Line of Sight

A NLOS link is rarely preferred over an LOS or partially obstructed LOS link, since NLOS links tend to have 10 to 50 dB more path loss and higher expected RMS delay spread. When the LOS direction is completely blocked by a building or other shadowing objects, the work here shows that a reflection, scattered, or diffraction path may still have sufficient signal strength to be received, albeit at a lower signal level. Distant-dependent propagation path-loss models were provided to account for LOS, NLOS, as well as the best possible path provided in NLOS conditions when using steerable antennas at the TX and RX.

**Experimental Result:** The Table 1 shows an experimental result of our work

### CONCLUSION

Given the worldwide need for cellular spectrum and the relatively limited amount of research done on mm-wave mobile communications, That have conducted extensive propagation measurement campaigns at 28 GHz and 38 GHz to gain insight on AOA, path loss and building penetration and reflection characteristics for the design of future mm-wave cellular systems. The base stations with a cell-radius of 200 meters. Path loss was larger in coefficients for outdoor materials were significantly higher, for example, 0.896 for tinted glass and 0.740 for clear non-tinted glass, compared with those of indoor building materials. Similarly, penetration losses were larger for outdoor material since signals cannot readily propagate through outdoor building materials, indoor networks will be isolated from outdoor networks and this suggests that data showers, repeaters and access points may need to be installed for handoffs at entrances of commercial and residential buildings. By observing the measured path loss and delay spread values from the heavy urban environment of and the light urban

environment. We found substantial differences in propagation parameters. Multipath delay spread is found to be much larger in urban environment due to the highly reflective nature of the dense urban environment. Small scale fading, a key factor for the design of urban cellular, has been tested and shows little change in received power and impulse response when highly directional antennas and 400 Mcps signals are used. The data collected over the course of these measurement campaigns allows for development of statistical channel models for urban environments and are highly valuable for the development of 5G cellular communications at mm-wave.

### REFERENCES

1. Pi, Z. and F. Khan, 2011. An introduction to millimeter-wave mobile broadband systems, *IEEE Commun. Mag.*, 49(6): 101-107.
2. Spatial Channel Model for Multiple Input Multiple Output (MIMO) Simulations (Release 10), Standard 3GPP TR 25.996, Mar. 2011.
3. Rappaport, T.S., Y. Qiao, J.I. Tamir, J.N. Murdock and E. Ben-Dor, 2012. Cellular broadband millimeter wave propagation and angle of arrival for adaptive beam steering systems (invited paper), in *Proc. IEEE Radio Wireless Symp.*, pp: 151-154.
4. Seidel, S.Y. and H.W. Arnold, 1995. Propagation measurements at 28 GHz to investigate the performance of local multipoint distribution service (LMDS), in *Proc. Global Telecommun. Conf.*, 1: 754-757.
5. Zhao, H., R. Mayzus, S. Sun, M. Samimi, J.K. Schulz, Y. Azar, K. Wang, G.N. Wong, F. Gutierrez and S.T. Rappaport, 2013. 28GHz millimeter wave cellular communication measurements for reflection and penetration loss in and around buildings in New York City, in *Proc. IEEE Int. Conf. Commun.*, pp: 1-6.
6. Rappaport T.S., T.S. Gutierrez, E. Ben-Dor, J.N. Murdock, Y. Qiao and J.I. Tamir, 2013. Broadband millimeter wave propagation measurements and models using adaptive beam antennas for outdoor urban cellular communications, *IEEE Trans. Antennas Propag.*, 61(4): 1850-1859.
7. Durgin, G., T.S. Rappaport and H. Xu. 1998. 5.85-GHz radio path loss and penetration loss measurements in and around homes and trees, *IEEE Commun. Lett.*, 2(3): 7072.
8. Zhao, Q. and J. Li, 2006. Rain attenuation in millimeter wave ranges, in *Proc. IEEE Int. Symp. Antennas, Propag. EM Theory*, pp: 1-4.

9. Cudak, M., A. Ghosh, T. Kovarik, R. Ratasuk, T. Thomas, F. Vook and P. Moorut, 2013. Moving towards mmwave-based beyond-4G (B-4G) Technology, in Proc. IEEE Veh. Technol. Soc. Conf., pp: 117.
10. Rusek, F., D. Persson, B. Lau, E. Larsson, T. Marzetta, O. Edfors and F. Tufvesson, 2013. Scaling up MIMO: Opportunities and challenges with very large arrays, IEEE Signal Process. Mag., 30(1): 40-60.
11. Rappaport, T.S., E. Ben-Dor, J.N. Murdock and Y. Qiao, 2012. 38 GHz and 60 GHz Angle-dependent Propagation for Cellular and peer-to-peer wireless communications, in Proc. IEEE Int. Conf. Commun., pp: 4568-4573.
12. Nokia Siemens Networks, 2011. 2020: Beyond 4G: Radio Evolution for the Gigabit Experience, Espoo.
13. Ericsson. 2011. LTE-A 4G Solution, Stockholm, Sweden [Online]. Available: [http://www.ericsson.com/news/110415\\_wp](http://www.ericsson.com/news/110415_wp)
14. P., 2010. Transition to 4G: 3GPP Broadband Evolution to IMT-Advanced (4G) [Online]. Available: <http://www.3gamerica.org>.
15. Nokia Siemens Networks, 2010. Long Term HSPA Evolution: Mobile Broadband Evolution beyond 3GPP Release 10, Espoo, Finland [Online].fg